A BOND GRAPH REPRESENTATION OF THE SAGITTAL SPINE FOR ESTIMATION OF RIDE COMFORT

Ali Akbari And Donald Margolis
HYUNDAI CENTER OF EXCELLENCE IN VEHICLE DYNAMIC SYSTEMS AND CONTROL
Department of Mechanical and Aerospace Engineering, UC Davis
Davis, California, 95616, USA
alakbari@ucdavis.edu & dlmargolis@ucdavis.edu

ABSTRACT

Biomechanical models are widely used in rehabilitation, posture prediction studies, and for injury risk assessment (Gatton, Pearcy, and Pettet 2011). With ride comfort becoming important to vehicle manufacturers, there's a demand for a universal, quantitative ride comfort metric (Da Silva 2002). Mechanical inputs from the ride to the passenger body could cause discomfort (ISO 1997) and the dominant discomfort-causing motions lie in the body's sagittal plane (longitudinal plane dividing a symmetrical body into left and right sections) (Kozawa, Sugimoto, and Suzuki 1986). This paper develops a biomechanical model of the sagittal spine using bond graphs. The model is computationally cost-effective as it employs fewer degrees of freedom than available models (Bazrgari, Shirazi-Adl, and Arjmand 2007; Amiri, Naserkhaki, and Parnianpour 2019) and is capable of estimating internal loads and displacements with sufficient accuracy. The model could be used for spinal load assessments and ride comfort studies in vehicle dynamics.

Keywords: Ride Comfort, Biomechanics, Sagittal Spine, Bond Graphs

1 INTRODUCTION

Passenger vehicle ride quality metrics have traditionally been subjective and sometimes contradictory (Jacklin 1936; Dieckmann 1958; Sperling and Betzhold 1957; Yang et al. 2009; Sharma 2016; Enders et al. 2019). The authors hypothesize that ride comfort can be correlated with the amount of motion induced in certain degrees of freedom of the passenger's body due to excitations from the seat. To estimate said motions, a sufficiently accurate biomechanical model of the sagittal spine is required. This paper develops such a model using bond graphs, including sufficient degrees of freedom for such study.

There have been biomechanical passenger models developed in the literature for studying vehicle seat or suspension (Gohari and Tahmasebi 2015; Wisner, Donnadieu, and Berthoz 1964). Most such models have exclusively studied the vertical motion within the body and have also treated the entirety of the body as a lump, with few internal degrees of freedom (Oncescu et al. 2020; Jamali Shakhlavi, Marzbanrad, and Tavoosi 2018; Cho and Yoon 2001; Guruguntla and Lal 2020). The passenger model will have to include the mechanical segments of the upper body, as it was demonstrated in (Kozawa, Sugimoto, and

ICBGM'2021 Nov 8-10, 2021- San Diego, California USA - ©2021 Society for Modeling & Simulation International (SCS)

Suzuki 1986) that it is input vibrations from the seat (and not the floor) that passengers feel the most. The human upper body's mechanical structure essentially consists of the human spine, which is stretched between the pelvis and the head (Tözeren 1999). Therefore, a biomechanical model of the human spine is developed in this study using bond graphs (Paynter 1958). To estimate passenger comfort in a cruising vehicle, a planar motion analysis in the sagittal plane would suffice, which includes two translational and one rotational degrees of freedom for each vertebra in the spinal column. This model could investigate how the vehicle's heave and pitch motions propagate through the spine. Using curvilinear coordinates in the sagittal plane, the model could express all planar motions for the spinal column. These motions include axial compression and bending rotation which are associated with chronic back pain; and transverse shear which indicates pressing on the spinal cord, which could lead to acute pain and, in extreme cases, paralysis. This model could later be integrated with various suspension control strategies and help determine which one induces the smallest internal motion, which represents the least pain, which in turn could be thought of as the highest comfort. The proposed bond graph model includes every bond graph element and could be used for a detailed study of planar biomechanics. Furthermore, such a model helps attain quantitative indexes for ride comfort instead of the traditional qualitative metrics.

Because of the spine's inherent curved S-shape (Ashton-Miller and Schultz 1997), even if it is only the vehicle's vertical vibration input that is to be considered, its mechanical effects within the body cannot be properly accounted for using a one-directional, vertical model. The spinal column itself is made up of three major vertebral sections, the lumbar spine (lowermost section), the thoracic spine (middle section), and the cervical spine (uppermost section) which are distinguished from one another according to changes in the direction of curvature of the spine (Ashton-Miller and Schultz 1997) as seen and named in Fig.1.

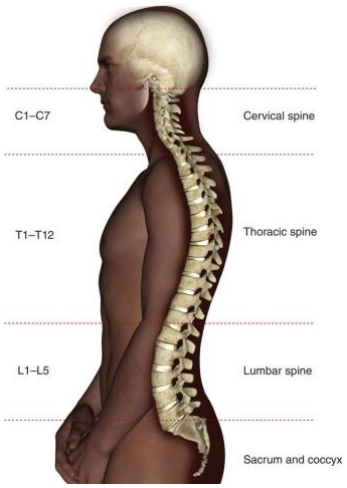

Figure 1. The Sagittal Spine and its built-in curvature, source: (https://radiologykey.com/spine-5/ 2016)

Decades-long studies have shown that lower-back pain, a medical condition involving the lumbar spine, is amongst the most common and costly musculoskeletal disorders (Webster and Snook 1994; Praemer, Furner, and Rice 1999). Amidst the three sections of the spine, the lumbar spine is prone to the highest chronic/acute pain (Praemer, Furner, and Rice 1999), is closest to the load input (hip cushion) for a vehicle's passenger (Abernethy et al. 1980), is under the highest weight portion of the upper body (De Leva 1996), and has the highest range of motion (Ashton-Miller and Schultz 1997). This makes the lumber spine be of utmost importance when building a biomechanical model of the upper body.

2 MODELING AND METHODS

2.1 Structure

The lumbar spine consists of 5 vertebrae called L1 through L5 and in between them there are intervertebral compliant discs which provide stiffness and damping (Ashton-Miller and Schultz 1997). According to (Kozawa, Sugimoto, and Suzuki 1986), the most prominent input motions from the seat to the body act within the vehicle's pitching plane which encompasses the vehicle's heave and

longitudinal translations, and its pitch rotation. In anatomical terms, that plane would be the body's sagittal plane with respective degrees of freedom (DOF) of axial displacement, shear displacement, and flexion/extension rotation. Hence, any vertebra or inertia has 3 DOFs in the sagittal plane. Due to its discussed sensitivity and importance, the lumbar spine is extensively modeled in this study with its internal vertebral degrees of freedom, compliances, resistances, and inertias. The thorax, however, is 10 times more massive than each lumbar vertebra (De Leva 1996). Because of being attached to the ribcage, the thoracic vertebrae are much more confined (higher intervertebral stiffness in the thoracic region); making the thoracic intervertebral motions be much smaller than that of the lumbar region in sagittal motions (Meakin et al. 2008). The cervical spine is not under much load (Walker, Harris, and Pontius 1973), and the neck in the sagittal plane is basically a hinge for the head's rotation (McGill et al. 1994).

Therefore, the thoracocervical spine will be modeled as a rigid thorax alongside a 3DOF joint for the neck. This rigid thorax+neck is in turn attached to a lump considered for the head. A schematic of the sitting passenger model is given in Fig.2.

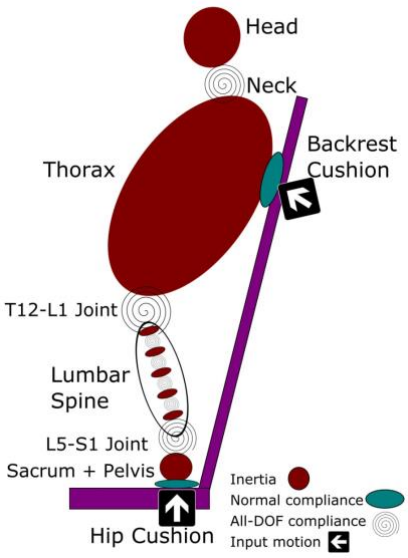

Figure 2. Schematic of the seated passenger model

This will make up for a 22-DoF model, including 7*3 DOFs for the 5 lumber vertebrae, the rigid thorax, and the head; in addition to one vertical degree of freedom for the sacrum and pelvis (the spine's "seat" rigidly attached to the hip).

Apart from the vertebrae which are modeled as inertias, and intervertebral discs which are modeled as spring and dampers; there are muscles, ligaments, and tendons attached to the vertebrae which are collectively soft tissue. They apply forces to the vertebrae and help with stabilizing the spine's motion. In this study, soft tissues are modelled as passive, rotary elements that apply restoring moments; as that is their most prominent effect in the sagittal motions of interest (Shirazi-Adl 2006).

A geometric schematic of the lower most section of the passenger model (Up until the L4 lumbar joint) is brought in Fig. 3, where the sprung mass vertical velocity is the input to the model which passes through the compliance of hip-cushion + buttocks. Pelvis is a rigid inertia which is the foundation on which the upper body essentially sits and can only move vertically. Then there are the first two lumbar vertebrae (L5-L4) and their intervertebral joints.

It's note-worthy that since the passenger model is essentially a tower of inertial elements with compliances In between them, the rest of the model repeats the same pattern; as thorax and head are assumed to be rigid and the same all-DOF compliance kind of joint will be modeled between the not-shown elements.

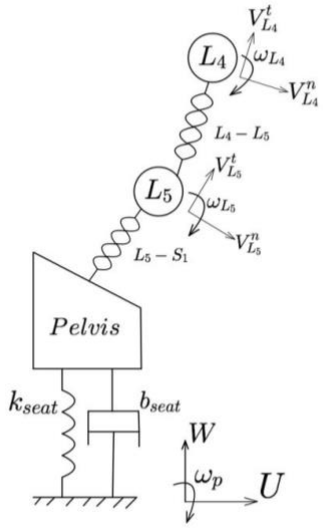

Fig 3. Schematic of the lowermost section of the passenger model

The input velocities to the passenger model come from the inertial vehicle frame and include U (longitudinal), and W (heave) velocities and the pitch angular velocity ω_p.

The intervertebral discs are modelled with all-degree compliances which are shown in Fig.3 with a rather non-conventional symbol. These elements will provide stiffness and damping for all modeled degrees of freedom, along the disc's axis for axial compression and perpendicular to it for shearing motion, as well as rotary compliance and resistance. Fig. 4 brings a schematic description of these elements.

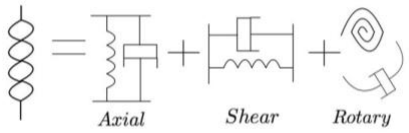

Figure 4. Schematic of the all-DOF compliance, used in modeling the intervertebral discs

2.2 Geometry

Fig.5 schematically shows two consecutive lumbar vertebrae (T and B subscripts refer to the Top and Bottom) along the spinal column with their velocities in body-fixed coordinates. Each inertial element has both tangential V_t and normal V_n translational velocities with respect to the spinal curve and an angular velocity ω in CCW rotation in the sagittal plane.

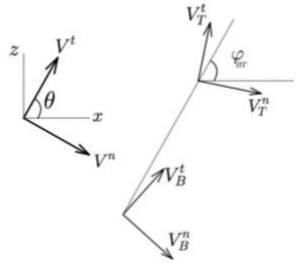

Figure 5. geometric diagram of two consecutive inertias T (top) and B (bottom), and their body-fixed coordinates

The tangential velocity direction makes an angle θ with the horizontal. The direction of the axial compliance for two consecutive vertebrae is taken to be that of the line that connects their centers of mass. The direction of the shear compliance is perpendicular to the axial direction towards positive curvature. The axial compliances make an angle φ with the horizontal. Each vertebra has its own θ but two consecutive vertebrae share a φ. The difference between θ and φ is defined as the ψ angle which is required for finding the components of compliance forces along tangential and normal directions for each vertebra.

By integrating the projections of the body-fixed velocities of each inertia in the inertial x and z directions, their inertial position will be found as:

$$x(t) = \int (V^t \cos\theta + V^n \sin\theta)dt + x_0 \qquad eq.(1)$$

$$z(t) = \int (V^t \sin\theta - V^n \cos\theta)dt + z_0 \qquad eq.(2)$$

Now the φ angle can be calculated as:

$$\tan\varphi_{TB} = \frac{z_T - z_B}{x_T - x_B} \qquad eq.(3)$$

The φ angles will be uniquely found since both the numerator and the denominator in the expression for its tangent are known and not just their ratio.

Since the equations of motion will be derived using bond graph modeling (Karnopp, Margolis, and Rosenberg 1990), it is necessary to find the components of the

vertebral velocities along compliance directions.

The tangential velocity vector makes an angle ψ with the direction of axial compliance, which is the same angle that the normal velocity makes with the direction of shear compliance and it is found as follows:

$$\psi_{TB} = \theta_T - \varphi_{TB}\ ;\ \psi_{BT} = \theta_B - \varphi_{TB} \qquad eq.(4-5)$$

2.3 Kinematics

The next step is to project the body-fixed velocities of two consecutive vertebrae along compliance directions to find the relative velocity across flexible elements. The velocity across compliant elements would be the relative velocity between the vertebrae's disc interfaces. Since vertebrae have a rather significant thickness (Ashton-Miller and Schultz 1997), the disc interface's velocity would not be the same as the center of mass's. Fig.6 schematically shows consecutive vertebrae with half-thicknesses D_B and D_T and their body-fixed velocities.

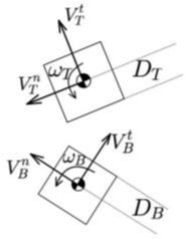

Figure 6. Velocity transfer from the center of mass to the disc interface due to vertebra thickness

Since the connecting displacement vector from the center of mass to the disc interface for each vertebra is in the tangential direction (with magnitude D_B or D_T), the interface (V_{int}) will have the same tangential velocity, and from velocity transfer its normal velocity would be equal to:

$$V_{B,int}{}^n = V_B{}^n + D_B\omega_B \qquad eq.(6)$$

$$V_{T,int}{}^n = V_T{}^n - D_T\omega_T \qquad eq.(7)$$

As the velocity vectors make the angle ψ with the compliance directions the interface velocity vectors are projected onto axial and shear compliance directions as follows:

$$\overrightarrow{V_T} = \left(V_T{}^t \cos\psi_{TB} - V_{T,int}{}^n \sin\psi_{TB}\right)\overrightarrow{e_a} + \left(V_T{}^t \sin\psi_{TB} + V_{T,int}{}^n \cos\psi_{TB}\right)\overrightarrow{e_s} eq.(8)$$

$$\overrightarrow{V_B} = \left(V_B{}^t \cos\psi_{BT} - V_{B,int}{}^n \sin\psi_{BT}\right)\overrightarrow{e_a} + \left(V_B{}^t \sin\psi_{BT} + V_{B,int}{}^n \cos\psi_{BT}\right)\overrightarrow{e_s} eq.(9)$$

Where $\overrightarrow{e_a}$, $\overrightarrow{e_s}$ represent the unit vectors for axial and shear directions, respectively. Now the relative velocity vector, positive in compression, across any intervertebral disc becomes:

$$\vec{V}_{rel,TB} = \overrightarrow{V_B} - \overrightarrow{V_T} = V_{rel,a}\overrightarrow{e_a} + V_{rel,s}\overrightarrow{e_s} \qquad eq.(10)$$

Also, the relative angular velocity vector across the discs, will be:

$$\omega_{rel,TB} = \omega_B - \omega_T \qquad eq.(11)$$

Now with the kinematics of the model figured out, one can move on to drawing the model's bond graph and deriving the equations of motion.

2.4 Bond Graphs

Bond Graph modeling (Paynter 1958; Karnopp and Rosenberg 1970; Karnopp, Margolis, and Rosenberg 1990) is a generalized approach to modeling dynamic systems through recognition of power transport in multi-domain systems. Since bong graph modelling is essentially an energy method, knowledge of the system's velocity configuration suffices for obtaining and solving the equations of motion, and one wouldn't need to investigate accelerations for the same purpose. Since there are too many states in the model for its bond graph to fit a page, the bond graph for a typical vertebra is given in Fig.7.

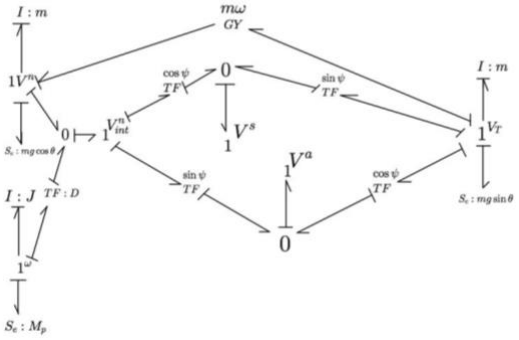

Figure 7. Bond Graph for a typical vertebra

This bond graph will be augmented with a complementary bond graph which connects two consecutive inertias, bringing in the compliances and resistances that act on each inertial element. The relative axial (V^a) and shear (V^s) velocities are represented as flow sources in the auxiliary bond graph in Fig.8.

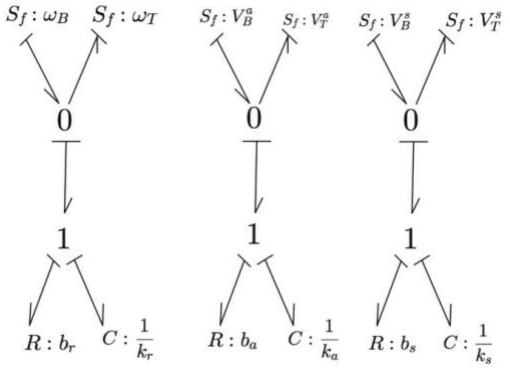

Figure 8. Complementary Bond Graph connecting two consecutive inertias

As noted in Fig.7 and Fig.8, the bond graphs are causal and equations of motion can be explicitly derived in integral causality.

2.5 Equations of Motion

The states variables in the model will be the velocities of the inertias in all their respective velocity directions: including tangential V^t, normal V^n, and rotational ω^r; and also the displacements of the compliances in their respective relative directions, namely axial q^a, shear q^s, rotational q^r, considered positive in compression.

Now the equations of motion for the top inertia are:

$$m\dot{V}_T{}^t = m_T\omega_T V_T{}^n + F_a\cos\psi_{TB} + F_s\sin\psi_{TB} - mg\sin\theta_T \quad eq.(12)$$

$$m\dot{V}_T{}^n = -m_T\omega_T V_T{}^t - F_a\sin\psi_{TB} + F_s\cos\psi_{TB} - mg\cos\theta_T \quad eq.(13)$$

$$J_T\dot{\omega}_T = M_r - M_{p_T} \quad eq.(14)$$

And for the bottom inertia:

$$m\dot{V}_B{}^t = m_B\omega_B V_B{}^n - F_a\cos\psi_{BT} - F_s\sin\psi_{BT} - mg\sin\theta_B \quad eq.(15)$$

$$m\dot{V}_B{}^n = -m_B\omega_B V_B{}^t + F_a\sin\psi_{BT} - F_s\cos\psi_{BT} - mg\cos\theta_B \quad eq.(16)$$

$$J_B\dot{\omega}_B = -M_r - M_{p_B} \quad eq.(17)$$

Where mentioned forces and moments are related to the state-space as follows:

$$F_a = k_a q_a + b_a V_{rel,a}\ ;\ F_s = k_s q_s + b_s V_{rel,s}\ ;\ M_r = k_r q_r + b_r\omega_{rel} \quad eq.(18-20)$$

$$\dot{q}_a = V_{rel,a}\ ;\ \dot{q}_s = V_{rel,s}\ ;\ \dot{q}_r = \omega_{rel} \quad eq.(21-23)$$

$$M_p = k_p\theta + b_p\omega \quad eq.(24)$$

In the given equations m, J indicate mass and sagittal moment of inertia for each body and D denotes their half-thickness. The parameters k, b designate stiffness and damping constants in their corresponding direction, respectively. The subscripts a, s, r indicate axial, shear, and rotary degrees of freedom, respectively. Also, the subscript p indicates the passive rotary reaction of the soft tissue pulling on the vertebrae.

2.6 Initial Conditions

The initial conditions for all velocities are zero and the initial condition for displacements are solved for using the steady state equations; since stable, linear dynamics systems achieve dynamic equilibrium at their static equilibrium position. Because of the spinal column's weight, all compliances are in an initial state of displacement. Also, the initial center of mass positions and the initial θ_0 angles are brought from literature (Pearsall, Reid, and Livingston 1996; De Leva 1996; Brodeur 1995; Bazrgari, Shirazi-Adl, and Arjmand 2007).

2.7 Validation and Parameter Investigation

Parameter values are extracted from literature; including values for all stiffness and damping constants (Keller, Colloca, and Béliveau 2002; Kasra, Shirazi-Adl, and Drouin 1992; Stokes et al. 2002; McGill et al. 1994; Markolf 1970; Owens Jr et al. 2007; Bazrgari, Shirazi-Adl, and Kasra 2008; Kim, Kim, and Yoon 2005; Guruguntla and Lal 2020; Oncescu et al. 2020; Cho and Yoon 2001; Jamali Shakhlavi, Marzbanrad, and Tavoosi 2018), as well as values for masses and moment of inertias (Pearsall, Reid, and Livingston 1996; De Leva 1996). An example of literature-investigated parameters is depicted in Fig. 9 which is brought from (Keller, Colloca, and Béliveau 2002).

Table 1
Summary of model flexible joint structure stiffness coefficients corresponding to the axial (x), transverse (y) and flexion–extension rotation (z) axes of each segment

Stiffness coefficient	Thorax	T12–L1	L1–L2	L2–L3	L3–L4	L4–L5	L5–L1	Pelvis and sacrum
k_x (kN/m)	1250	640	620	600	525	450	510	300
k_y (kN/m)	30	50	40	35	30	30	45	200
κ_z (Nm/rad)	400	160	140	120	100	80	75	700

Figure 9. Typical stiffness values for all degrees of freedom employed in the model. Source: (Keller, Colloca, and Béliveau 2002)

However, it has been noted that most values reported in the literature for stiffness and damping parameters are rather discrepant, as their corresponding testing experiments and their respective settings have not been the same for each investigated parameter. Therefore, the best set of parameters that complies best with results from literature on the internal motion of the body needs to be investigated. This effort will validate the model against available experimental results and makes sure that the motion the model will predict will be reasonable.

3 RESULTS AND DISCUSSION

The model was simulated with an initial velocity excitation of 1.8414 m/s at the location of the L3 vertebra in the normal direction, which is the excitation employed in Keller et al.'s simulation study for lumbar spinal loads (Keller, Colloca, and Béliveau 2002). Fig. 10 through Fig.12 depict the displacements for the L3-L4 motion segment in response to said excitation.

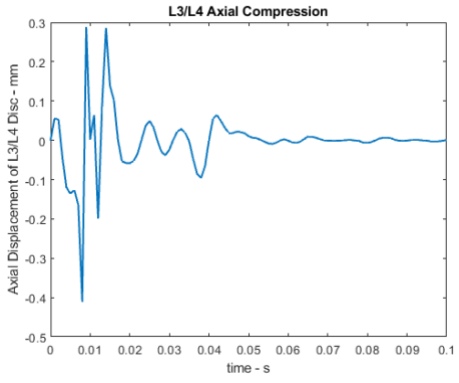

Figure 10. L3/L4 segment's axial compression

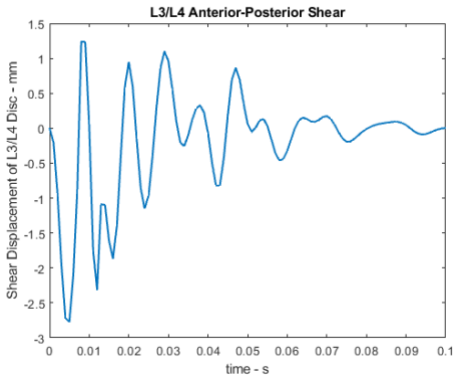

Figure 11. L3/L4 segment's shear displacement

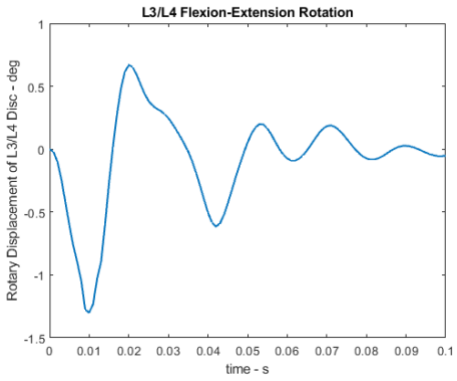

Figure 12. L3/L4 segment's rotary displacement

The given displacement profiles have peak-to-peak values of 0.7mm, 3.5mm, and 1.8 degrees; which correspond closely to the predicted values by (Keller, Colloca, and Béliveau 2002). This serves as a preliminary validation for the passenger model and suggests that its predicted results are reasonable.

4 FUTURE WORK

To ensure the model's accuracy in predicting the internal motions of the body, it needs to be further validated both statically and dynamically. Static validation will be against (Wilke et al. 1999), which is a unique in-vivo experiment that reports the intradiscal pressure of the fluid within the L4/L5 disc, which is proportional to the axial compressive force in that disc, for various activities and postures. Furthermore, the model will be dynamically validated against simulation models that predict natural frequencies, damping ratios, and transient responses for the sagittal spine

such as (Zirbel et al. 2013; Wang et al. 2010).

5 CONCLUSION

There is yet a demand for a quantitative, universal ride comfort metric. This paper approaches this problem from a biomechanical perspective by hypothesizing that the ideal ride is that which induces the least internal motion within a passenger's body. For this purpose, a biomechanical model of the sagittal spine is developed with axial, shear, and rotary degrees of freedom. The model incorporates a novel geometry which enables accounting for the spinal curvature and its curved motion. The model is validated against available literature for reasonable range of motion. Future studies could implement the model in their investigation to come up with ride-comfort-enhancing suspension or seat designs for autonomous vehicles.

6 REFERENCES

Abernethy, CN, HH Jacobs, GR Plank, JH Stoklosa, and ED Sussman. 1980. "Maximum deceleration and jerk levels that allow retention of unrestrained, seated transit passengers." *Evaluation* 1 (10).

Amiri, Sorosh, Sadegh Naserkhaki, and Mohamad Parnianpour. 2019. "Effect of whole-body vibration and sitting configurations on lumbar spinal loads of vehicle occupants." *Computers in biology and medicine* 107:292-301.

Ashton-Miller, James A, and Albert B Schultz. 1997. "Biomechanics of the human spine." *Basic orthopaedic biomechanics* 2:353-385.

Bazrgari, B, A Shirazi-Adl, and M Kasra. 2008. "Computation of trunk muscle forces, spinal loads and stability in whole-body vibration." *Journal of Sound and Vibration* 318 (4-5):1334-1347.

Bazrgari, Babak, Aboulfazl Shirazi-Adl, and Navid Arjmand. 2007. "Analysis of squat and stoop dynamic liftings: muscle forces and internal spinal loads." *European Spine Journal* 16 (5):687-699.

Brodeur, Raymond R. 1995. "Modeling spine shape for the seated posture." *Spine* 1 (L5):T12.

Cho, Younggun, and Yong-San Yoon. 2001. "Biomechanical model of human on seat with backrest for evaluating ride quality." *International Journal of Industrial Ergonomics* 27 (5):331-345.

Da Silva, MC Gameiro. 2002. "Measurements of comfort in vehicles." *Measurement Science and Technology* 13 (6):R41.

De Leva, Paolo. 1996. "Adjustments to Zatsiorsky-Seluyanov's segment inertia parameters." *Journal of biomechanics* 29 (9):1223-1230.

Dieckmann, D. 1958. "A study of the influence of vibration on man." *Ergonomics* 1 (4):347-355.

Enders, Erik, Georg Burkhard, Felix Fent, Markus Lienkamp, and Dieter Schramm. 2019. "Objectification methods for ride comfort." *Forschung im Ingenieurwesen* 83 (4):885-898.

Gatton, Michelle L, Mark J Pearcy, and Graeme J Pettet. 2011. "Computational model of the lumbar spine musculature: implications of spinal surgery." *Clinical Biomechanics* 26 (2):116-122.

Gohari, Mohammad, and Mona Tahmasebi. 2015. "Active off-road seat suspension system using intelligent active force control." *Journal of Low Frequency Noise, Vibration and Active Control* 34 (4):475-489.

Guruguntla, Veeresalingam, and Mohit Lal. 2020. "An Improved Biomechanical Model to Optimize Biodynamic Responses Under Vibrating Medium." *Journal of Vibration Engineering & Technologies*:1-11.

https://radiologykey.com/spine-5/. 2016. "Radiology Key website." https://radiologykey.com.

ISO. 1997. ISO 2631-1:1997(E). In *Mechanical Vibration and Shock - Evaluation of Human Exposure to Whole-Body Vibration*. Geneva, International Organization for Standardization: Geneva, International Organization for Standardization.

Jacklin, HM. 1936. "Human reactions to vibration." *SAE Transactions*:401-408.

Jamali Shakhlavi, Somaye, Javad Marzbanrad, and Vahid Tavoosi. 2018. "Various vehicle speeds and road profiles effects on transmitted accelerations analysis to human body segments using vehicle and biomechanical models." *Cogent Engineering* 5 (1):1461529.

Karnopp, Dean C, Donald L Margolis, and Ronald C Rosenberg. 1990. "System dynamics." *Modeling and simulation of mechatronic systems* 4.

Karnopp, Dean, and Ronald C Rosenberg. 1970. "Application of bond graph techniques to the study of vehicle drive line dynamics."

Kasra, M, A Shirazi-Adl, and G Drouin. 1992. "Dynamics of human lumbar intervertebral joints. Experimental and finite-element investigations." *Spine* 17 (1):93-102.

Keller, Tony S, Christopher J Colloca, and Jean-Guy Béliveau. 2002. "Force-deformation response of the lumbar spine: a sagittal plane model of posteroanterior manipulation and mobilization." *Clinical biomechanics* 17 (3):185-196.

Kim, Tae-Hyeong, Young-Tae Kim, and Yong-San Yoon. 2005. "Development of a biomechanical model of the human body in a sitting posture with vibration transmissibility in the vertical direction." *International Journal of Industrial Ergonomics* 35 (9):817-829.

Kozawa, Yoshihiko, Gunji Sugimoto, and Yasuhiko Suzuki. 1986. "A new ride comfort meter." *SAE Transactions*:1038-1045.

Markolf, Keith L. 1970. "Stiffness and damping characteristics of the thoracolumbar spine." Proceedings of workshop on bioengineering approaches to problems of the spine. Division of Research Grants, NIH, Bethesda.

McGill, SM, K Jones, G Bennett, and PJ Bishop. 1994. "Passive stiffness of the human neck in flexion, extension, and lateral bending." *Clinical Biomechanics* 9 (3):193-198.

Meakin, Judith R, Jennifer S Gregory, Francis W Smith, Fiona J Gilbert, and Richard M Aspden. 2008. "Characterizing the shape of the lumbar spine using an active shape model: reliability and precision of the method." *Spine* 33 (7):807-813.

Oncescu, AT, D Tarnita, D Bolcu, and R Malciu. 2020. "A study of biomechanical model of seated human body exposed to vertical vibrations." IOP Conference Series: Materials Science and Engineering.

Owens Jr, Edward F, James W DeVocht, M Ram Gudavalli, David G Wilder, and William C Meeker. 2007. "Comparison of posteroanterior spinal stiffness measures to clinical and demographic findings at baseline in patients enrolled in a clinical study of spinal manipulation for low back pain." *Journal of manipulative and physiological therapeutics* 30 (7):493-500.

Paynter, HM. 1958. "Generalizing the concepts of power transport and energy ports for system engineering." ASME Presented at the 1958 Annual Meeting New York. NY.

Pearsall, David J, J Gavin Reid, and Lori A Livingston. 1996. "Segmental inertial parameters of the human trunk as determined from computed tomography." *Annals of biomedical engineering* 24 (2):198-210.

Praemer, Allan, Sylvia Furner, and Dorothy P Rice. 1999. *Musculoskeletal conditions in the United States*: American Academy of Orthopaedic Surgeons.

Sharma, Rakesh Chandmal. 2016. "Evaluation of Passenger Ride Comfort of Indian Rail and Road Vehicles with ISO 2631-1 Standards: Part 2-Simulation." *International Journal of Vehicle Structures & Systems (IJVSS)* 8 (1).

Shirazi-Adl, A. 2006. "Analysis of large compression loads on lumbar spine in flexion and in torsion using a novel wrapping element." *Journal of biomechanics* 39 (2):267-275.

Sperling, Eo, and C Betzhold. 1957. "Contribution to evaluation of comfortable running of railway vehicles." Bulletin of the International Railway Congress Association.

Stokes, Ian A, Mack Gardner-Morse, David Churchill, and Jeffrey P Laible. 2002. "Measurement of a spinal motion

segment stiffness matrix." *Journal of biomechanics* 35 (4):517-521.
Tözeren, Aydin. 1999. *Human body dynamics: classical mechanics and human movement*: Springer Science & Business Media.
Walker, Leon B, Edward H Harris, and Uwe R Pontius. 1973. Mass, volume, center of mass, and mass moment of inertia of head and head and neck of human body. SAE Technical Paper.
Wang, Wenping, Babak Bazrgari, Aboulfazl Shirazi-Adl, Subhash Rakheja, and Paul-Emile Boileau. 2010. "Biodynamic response and spinal load estimation of seated body in vibration using finite element modeling." *Industrial health* 48 (5):557-564.
Webster, Barbara S, and Stover H Snook. 1994. "The cost of 1989 workers' compensation low back pain claims." *Spine* 19 (10):1111-1115.
Wilke, Hans–Joachim, Peter Neef, Marco Caimi, Thomas Hoogland, and Lutz E Claes. 1999. "New in vivo measurements of pressures in the intervertebral disc in daily life." *Spine* 24 (8):755-762.
Wisner, A, A Donnadieu, and A Berthoz. 1964. "A biomechanical model of man for the study of vehicle seat and suspension." *The International Journal of Production Research* 3 (4):285-315.
Yang, Yong, Weiqun Ren, Liping Chen, Ming Jiang, and Yuliang Yang. 2009. "Study on ride comfort of tractor with tandem suspension based on multi-body system dynamics." *Applied Mathematical Modelling* 33 (1):11-33.
Zirbel, Shannon A, Dean K Stolworthy, Larry L Howell, and Anton E Bowden. 2013. "Intervertebral disc degeneration alters lumbar spine segmental stiffness in all modes of loading under a compressive follower load." *The Spine Journal* 13 (9):1134-1147.

AUTHOR BIOGRAPHIES

ALI AKBARI is a PhD student of Mechanical Engineering at UC Davis where he researches ride comfort for vehicle occupants at Hyundai Center of Excellence. He received his BSc and MSc from Sharif University of Technology with a focus in biomechanics. His email address is alakbari@ucdavis.edu .

DONALD L. MARGOLIS is a professor of mechanical engineering and director of the Hyundai Center of Excellence in Vehicle Dynamics Systems & Control at UC Davis. He has extensive experience in teaching system dynamics at the graduate and undergraduate levels, consultation in vibration controls, and has published numerous papers on the industrial applications of dynamics. His email is dlmargolis@ucdavis.edu.